Developmental regulation of oocyte lipid uptake via 'patent' follicular epithelium in *Drosophila melanogaster*

Sarayu Row[1] and Wu-Min Deng*[1,2]

Affiliations

[1]Department of Biological Science, Florida State University, Tallahassee, FL 32306-4295, USA

[2]Department of Biochemistry and Molecular Biology, Tulane University School of Medicine, New Orleans, LA 70112, USA

*Correspondence to: wdeng7@tulane.edu

Abstract

Epithelia form protective permeability barriers that selectively allow the exchange of material while maintaining tissue integrity under extreme mechanical, chemical, and bacterial loads. Here, we report in the *Drosophila* follicular epithelium a developmentally regulated and evolutionarily conserved process, 'patency', wherein a breach is created in the epithelium at tricellular contacts during mid-vitellogenesis. In *Drosophila*, patency exhibits a strict temporal range delimited by the transcription factor Tramtrack69, and a spatial pattern regulated by the dorsal-anterior signals of the follicular epithelium. Crucial for lipid uptake by the oocyte, patency is also exploited by endosymbionts such as *Spiroplasma pulsonii*. Our findings reveal an evolutionarily conserved non-typical epithelial function in a classic model system.

Introduction

Epithelial integrity is maintained through cell division, apoptosis, and morphogenetic movements *(1,2)*, and the preservation of tricellular contacts (TCs) is key to its physical and electrochemical barrier function *(3)*. Failure to maintain TCs can disrupt epithelial integrity and have catastrophic consequences such as metastatic cancer *(4,5)* and Crohn's disease *(6)*. The epithelium is also permeable, allowing selective passage of material via transcellular and paracellular routes *(7)*. The extensively characterized *Drosophila* follicular epithelium (FE) surrounding developing egg chambers provides an excellent model to study the balance between barrier function and permeability in epithelia. As the developmental unit of oogenesis, each egg chamber is comprised of an oocyte and 15 nurse cells, all enclosed in the FE monolayer (*8*). A string of sequentially developing egg chambers beginning with the germarium and advancing from stages 1 through 14 is contained in each of the 16 ovarioles in each 'meroistic' ovary (*8)* [Fig. 8.]. The

47 FE monolayer protects and supports germline development while going through a series of
48 spatiotemporally regulated morphogenetic movements, and also secretes the chorion, or eggshell
49 *(8, 9)*. Vitellogenic stages (stage (St) 8-12) are characterized by the trans-epithelial movement of
50 hemolymph-borne yolk proteins (YPs) into the oocyte. YPs are synthesized primarily in the fat
51 body, secreted into the hemolymph, and travel between the follicle cells to reach the oocyte
52 membrane, and are internalized via receptor-mediated endocytosis *(10-12)*. The FE also
53 synthesizes YPs in small amounts until St 11 when it switches to chorion secretion *(13, 14)*.
54 Other materials carried by the hemolymph have been postulated to enter the oocyte, such as
55 lipophorins and endosymbionts *(15,16)*, but the mechanistic details of trans-epithelial FE
56 transport remain unclear.
57 In this study, we present a mechanism for the trans-epithelial transport of lipids across the FE, a
58 phenomenon termed 'patency', previously unreported in *Drosophila*. Unlike in other insects, we
59 found that patency in *Drosophila* is only present in mid-vitellogenesis. This reduced temporal
60 range appears to be regulated by the BTB transcription factor Tramtrack69 (Ttk69). We also
61 report a consistent spatial pattern of patency in the FE, influenced by the signaling pathways that
62 pattern the dorsal anterior. Moreover, we found the spatiotemporal patterns of patency are
63 evolutionarily conserved in the *Drosophila* species. Together, our results reveal a
64 developmentally regulated function of the follicular epithelial tissues, wherein a breach is created
65 for trans-epithelial material transfer.
66
67 **Results**
68 *Drosophila* follicular epithelium exhibits patency

69 While examining wildtype (WT) *Drosophila melanogaster* egg chambers, we noticed an
70 anomalous but consistent feature — the opening of the TCs in mid-vitellogenic FE. These TC
71 'gaps' are present at the basal, lateral, and apical domains of the FE [Fig. 1(A-D"), Fig. S1(B),
72 (D-H)], effectively creating a breach in the epithelium. Although not previously described in
73 *Drosophila*, several insect species have been reported to exhibit 'patency', a phenomenon
74 characterized by the opening of intercellular contacts between follicle cells for oocyte yolk
75 uptake during vitellogenesis *(17)*. We confirmed the appearance of TC gaps using a milder
76 detergent-free immunostaining protocol, as well as electron microscopy [Fig. S1(A-A"), Fig.
77 1(E-E')], demonstrating that *Drosophila* FE indeed exhibits patency.

78 <u>Temporal range of patency and regulation by Ttk69</u>

79 Unlike in other insects (e.g., *R. proxilus*) where patency is present in most vitellogenic stages
80 *(18)*, we found that patent TCs in *Drosophila* FE are present only during mid-vitellogenic stages
81 (St10a and 10b), suggesting a more limited temporal range [Fig. 2(A-E")]. Immunostaining with
82 various epithelial markers revealed a dynamic pattern of junction and adhesion proteins in the
83 TCs over the course of patency [Fig. S2(A-T")]. Septate junctions, marked by Discs large (Dlg),
84 lose their connections at TCs during patent stages and are reconnected at stage 11 when the gaps
85 disappear [Fig. S2(A-D")]. Adherens junctions, represented by E-cadherin (E-cad), are removed
86 from TCs in patent epithelia, and reappear when patency is terminated [Fig. S2(E-H")]. In
87 contrast, cortical F-actin remains intact and continuous through mid-vitellogenesis, although
88 marginally reduced, indicating that the structural integrity might not be compromised even in
89 patent FE [Fig. S2(I-L")]. The tricellular junction (TCJ) septate junction protein Gliotactin (Gli)
90 (*19*), however, only appears at the TCs starting at late stage 10b [Fig. S2(M-P")], coincident with
91 the cessation of patency. The accumulation of Gli at TCs suggests the assembly of the TCJs - at

92 least the tricellular septate junctions - at the termination of patency, tipping the functional
93 balance of the FE away from trans-epithelial transport, and in favor of barrier function for the
94 remainder of oogenesis. Additionally, the extracellular matrix protein Laminin accumulates in
95 the gaps at St 10b [Fig. S2(Q-T"')], indicating the possibility of basement membrane
96 components also being transported across the epithelium, perhaps to aid in the closing or
97 maintenance of the TCs post-patency. Consistent staging of egg chambers was based on Jia *et*
98 *al*., 2015 (*20*).
99 Next, to determine how patency is temporally regulated, we performed an RNAi screen for
100 transcription factors known to be active during mid-oogenesis, and identified Ttk69 - a zinc-
101 finger transcription factor that coordinates FE morphogenesis by regulating the expression levels
102 and localization of adhesion proteins such as E-Cad *(21, 22)*. Ttk69, previously reported to be
103 expressed starting at St 10a, is also expressed during pre- and early vitellogenic stages [Fig.
104 S3(A-D')], and knocking down *ttk69* resulted in a larger temporal range of patency, with ectopic
105 TC gaps ranging from St 9-11 [Fig. 3(A-D"")]. Similar to normal patent FE [Fig. S2(F-G")],
106 *ttk69*-knockdown FE with premature patency exhibited a lack of E-cad at TCs [Fig. S3(E-F'")],
107 suggesting that Ttk69 plays a role in restricting the temporal range of patency in the FE.

108 <u>Spatial pattern of patency is influenced by the dorsal anterior signals of the FE</u>
109 While examining St 10b egg chambers, we discovered that patency also shows a spatial pattern
110 in the FE - specifically, the dorsal-anterior region has intact TCs while the rest of the FE TCs are
111 patent at St 10b [Fig. 4(A-B'", G-G')]. The *Drosophila* FE is patterned along the anteroposterior
112 and dorsoventral axes by the BMP (Bone Morphogenetic Protein) or Decapentaplegic (Dpp), and
113 Epidermal Growth Factor Receptor (EGFR) pathways, creating a well-characterized subset of
114 cells in the dorsal anterior with elevated levels of adhesion proteins (eg., E-cad, Fasciclin 3

115 (Fas3)) *(23-25)* [Fig. S4(A-B’’’)]. Ectopic expression of Dpp in the whole FE resulted in elevated
116 E-cad and Fas3 levels across the FE [Fig. S4(F-G”)], and all TCs remained intact at St 10a [Fig.
117 4(C-D”, H-H’)]. In contrast, removal of EGF signaling by expressing a dominant negative form
118 of EGFR in the FE resulted in the loss of E-cad and Fas3, and ectopic patency in the dorsal
119 anterior FE, thus eliminating the spatial pattern of patency [Fig. S4(H-I”), Fig. 4(E-F”, I-I’)].
120 Together, our data indicate that the spatial distribution of patency in the FE is largely regulated
121 by Dpp and EGFR signaling.

122 <u>Patency is required for oocyte lipid uptake, and assists in vertical transfer</u>

123 During oogenesis, lipid levels show a marked increase in the oocyte at St 10a *(26)*, which,
124 incidentally, is also when TC gaps appear in the FE, and we therefore hypothesized that lipids
125 are transferred across the FE into the oocyte via patency. Indeed, our TEM pictures showed
126 material that could possibly be lipids in the gaps of patent FE [Fig. S1(C)]. Further investigation
127 using neutral lipid dyes Nile red and BODIPY revealed that lipids were in fact present in the TC
128 gaps, and appeared to be moving across the epithelium through the gaps [Fig. 5(A-C’’’’)].
129 Additionally, in egg chambers with FE lacking patency, the oocyte lipid levels were significantly
130 reduced at St 10a [Fig. 5(D-E”)], suggesting that follicular patency is necessary for oocyte lipid
131 uptake. Consistently, egg chambers which develop with FE lacking patency appear to be
132 abnormal, with a smaller oocyte at later stages, in addition to the expected lack of dorsal
133 appendages as a consequence of ectopic *UAS-Dpp* expression [Fig. 5(F-F’)].
134 Recently, the hormone ecdysone was shown to induce lipid uptake at St 10a by an unknown
135 mechanism *(26)*. When we expressed a dominant negative form of the ecdysone receptor EcR
136 B1, the FE showed no signs of patency [Fig. S5]. Along with our lipid data, we thus propose that

137 patency is the mechanism by which the St 10a oocyte accumulates lipids under ecdysone
138 regulation.
139 Endosymbionts also enter the oocyte from the maternal hemolymph in mid-vitellogenesis (*16),*
140 and we asked whether patency assists in this vertical transfer. Staining egg chambers for the
141 endosymbiont *Spiroplasma pulsonii*, we found that some bacteria are present between the follicle
142 cells prior to the onset of patency, while heavily populating the TC gaps at St 10a and 10b (*16*)
143 [Fig. 6(A-B")]. In FE lacking patency, *S. poulsonii* was still detected between the follicle cells as
144 in earlier stages of vitellogenesis [Fig. 6(C-D")]. These data suggest that patency is an advantage
145 rather than a dependence for vertical transmission.
146 <u>*D. simulans* FE presents similar spatiotemporal patterns of patency</u>
147 To determine whether the temporal range and spatial pattern of patency are unique to *D.*
148 *melanogaster*, we examined the ovaries of the closely related species *Drosophila simulans*. The
149 FE of only St 10a and St 10b egg chambers have patent TCs in *D. simulans* as well [Fig. 7(A-
150 D''')]. The oocyte associated FE of St 10b egg chambers in *D. simulans* also presented a similar
151 spatial pattern of patency as in *D. melanogaster,* with intact TCs in the dorsal anterior region
152 [Fig. 7(E-F")]. Together, our data indicates that the temporal and spatial patterns of patency
153 could be evolutionarily conserved.
154
155 **Discussion**
156 In this study, we report that *Drosophila melanogaster* exhibits a phase in oogenesis when the
157 oocyte-associated follicular epithelium develops 'gaps' that extend across the monolayer,
158 creating a breach in the epithelium, a process referred to as 'patency'. The FE, whose primary
159 function is to maintain an intact shield around the egg chamber, is developmentally perforated

160 with TC gaps essential for lipid transport. We illustrate spatiotemporal regulation of patency on a
161 global scale by the ecdysone signal, at a local level by the axial patterning signals of the FE (Dpp
162 and EGFR), and at a transcriptional level by Ttk69. These signals together regulate TC openings
163 to allow trans-epithelial transport of lipids [model in Fig. 8].
164 The use of *CY2-Gal4* to drive the expression of genes vital for vitellogenic progression allowed
165 us to tease out patent-stage specific effects of the regulators on the FE. For instance, our data
166 showing the requirement of the Ecdysone signal for the formation of patent TCs [Fig. S5]
167 suggests an important new role for the steroid hormone both temporally and functionally. In
168 several insects such as *R. proxilus*, *L. migratoria*, and *T. castaneum*, the sesquiterpenoid juvenile
169 hormone (JH) has been reported to be a major regulator of patency (*27-29*). A complex
170 interaction between the two hormones coordinates vitellogenic progression in *Drosophila* (*30,*
171 *31*). It is, therefore, possible that patency in *Drosophila* could also be affected by JH, as well as
172 its interaction with Ecdysone. Although Ttk69 is placed directly downstream of Ecdysone
173 activation in later oogenesis *(22)*, our data suggests a more complex interaction for the regulation
174 of patency.
175 While characterizing the junctions across patent stages, we observed the presence of Gli at the
176 cessation of patency. Gli, although a central component of TCJ septate junctions (*19*), is only one
177 component of the TCJs in epithelia. Other known TCJ proteins and assemblers include
178 Anakonda (Aka), the master regulator of Gli expression and localization (*32*), Sidekick, the
179 tricellular junction adherens junction protein (*33-35*), and M6, the TCJ protein required for
180 oogenesis (*36*). It is possible that these and other TCJ proteins might be involved in the creation,
181 maintenance, and termination of patency in the FE. An assessment of the chronological order of

182 appearance, localization, and expression levels over the course of patency, in addition to
183 functional studies, will help delineate the mechanistic details of patency in the FE.
184 A previous report on tissue remodeling via a non-canonical secretion pathway aids in closing
185 'open Zones of contact (ZOCs)', and we propose that these open ZOCs are indeed the patent TCs
186 we have characterized here *(37)*. Furthermore, our *D. simulans* data show that the temporal range
187 of patency and its spatial pattern could be evolutionarily conserved. Further analysis of patency
188 in other insects will ascertain whether the spatiotemporal patterns are evolutionarily conserved,
189 specifically in meroistic ovaries similar to those of *D. melanogaster* and *D. simulans*. Altogether,
190 this study creates a platform for further research into epithelial behavior, TCJ assembly and
191 dynamics, and trans-epithelial transport mechanisms.
192

193 **Methods**

194 *Drosophila* strains and culture

195 All *Drosophila* stocks were maintained and crossed at 21–22°, unless otherwise indicated. The
196 w[118] strain was used as the wild-type control. To control the temporal and regional gene
197 expression targeting (TARGET) system, temperature-sensitive Gal80 ($Gal80^{TS}$) under the
198 ubiquitous tubulin driver was used to regulate the upstream activating sequence (UAS)-transgene
199 expression by altering temperatures. *Tj-Gal4* and *CY2-Gal4* were used to drive UAS transgene
200 expression in combination with $Gal80^{TS}$. The crosses involving $Gal80^{TS}$ were crossed and
201 maintained at 18˚C, and progeny were kept at 29˚C for 48hrs prior to dissection.

202 Tj-Gal4 is used to drive transgenes under UAS control in all the follicle cells across oogenesis.
203 Transgenes that disrupt vitellogenic progression were used with *CY2-Gal4*, that drives transgenes

204 under UAS control in only the oocyte associated follicle cells starting at low levels at St 9, and
205 at high levels from St 10a [Fig. S4.(C-E')].

206 The following stocks were used: w[118] (Bloomington Drosophila stock Center (BDSC) #5905),
207 *UAS Gli RNAi* (RNA interference) (BDSC #58115), *UAS ttk RNAi* (BDSC #27325), *UAS Dpp*
208 (BDSC #1486), *Tj-Gal4* (BDSC #4775), *CY2-Gal4* (a gift from Dr. Berg), a*lphaTub84B-Gal4,*
209 *UAS-mCD8:GFP* (BDSC#30030), *UAS EGFR DN* (BDSC #5364), *10XUAS-IVS-myr::td Tomato*
210 (BDSC #32221), *UAS EcR B1 DN* (BDSC #6872), *D. Simulans* (a gift from Dr. Houle).

211 Immunostaining and fluorescence microscopy

212 Ovaries were dissected, fixed, and stained with antibodies as described previously (*38, 39*). The
213 following primary antibodies were used: Hu li tai shao (Hts) (1:5, 1B1), E-cadherin (Ecad) (1:20,
214 DCAD2), Discs large (Dlg) (1:50, 4F3), and Fasciclin3 (Fas3) (1:15, 7G10) all from the
215 Developmental Studies Hybridoma bank (DSHB), Laminin (gamma 1) (1:200, ab47651,
216 Abcam), Gliotactin (1:50, a gift from Dr. Auld), MSRO (1:200, a gift from Dr. Lemaitre), Ttk69
217 (1:200, a gift from Dr. Xi). Alexa Fluor 488- or 546-conjugated goat anti-mouse and anti-rabbit
218 secondary antibodies (1:400; Molecular Probes, Eugene, OR) were used. Phalloidin-546
219 (Invitrogen) was used to stain F-actin. Nuclei were labeled with DAPI (1:1000). Images were
220 captured with Zeiss LSM 800 confocal microscope. Zeiss and ImageJ software were used for
221 image analyses and processing.

222 Detergent-free protocol was modified from the standard protocol above, with all the same
223 reagents prepared without Tween-20.

224 Lipid staining with Nile red and BODIPY: Ovaries were dissected in PBS and fixed in 4% PFA
225 for 15 minutes. Following 2 washes with PBT, the ovaries were incubated in Nile red (TCI

226 America, 7385-67-3) (0.002% dye diluted in PBT, adopted from 29) or BODIPY 493/503
227 (ThermoFisher Scientific, Cat No. D3922) (Stock: 1mg/ml BODIPY in absolute ethanol,
228 Working: 1:500 in PBS) in dark for 30 minutes. Following 2 PBT washes, the ovaries were
229 either stained with antibodies, or with DAPI and then mounted onto slides.

230 Transmission Electron Microscopy

231 The samples for TEM were prepared as previously described (*40, 41*). Tissue samples were fixed
232 with Karnovsky's Fixative. After three rinses with 0.1 M sodium cacodylate buffer, samples were
233 embedded in 3% agarose and sliced into small blocks (1mm3), rinsed with the same buffer three
234 times and post-fixed with 1% osmium tetroxide and 0.8 % Potassium Ferricyanide in 0.1 M
235 sodium cacodylate buffer for one and a half hours at room temperature. Samples were rinsed
236 with water and en bloc stained with 4% uranyl acetate in 50% ethanol for two hours. They were
237 then dehydrated with increasing concentration of ethanol, transitioned into propylene oxide,
238 infiltrated with Embed-812 resin and polymerized in a 60°C oven overnight. Blocks were
239 sectioned with a diamond knife (Diatome) on a Leica Ultracut 7 ultramicrotome (Leica
240 Microsystems) and collected onto copper grids, post stained with 2% aqueous Uranyl acetate and
241 lead citrate. Images were acquired on a JEM-1400 Plus transmission electron microscope
242 equipped with a LaB6 source operated at 120 kV using an AMT-BioSprint 16M CCD camera.
243

244 **Data Availability**

245 All data generated or analyzed during this study are included in this manuscript and the
246 supplementary information files.
247

248 **References**

1. Guillot, C. & Lecuit, T. Mechanics of Epithelial Tissue Homeostasis and Morphogenesis, *Science*, **340**, 1185-1189 (2013).
2. Tai, K., Cockburn, K., & Greco, V. Flexibility sustains epithelial tissue homeostasis. *Curr Opin Cell Biol.,* **60**, 84–91 (2019).
3. Bosveld, F., Wang, Z., & Bellaïche, Y. Tricellular junctions: a hot corner of epithelial biology, *Curr opin Cell Biol*, ***54***, 80–88 (2008).
4. Jang, C., Starz-Gaiano, M., & Montell, D. J. Modeling migration and metastasis in *Drosophila*. *J Mammary Gland Biol Neoplasia*, **12**, 103–114 (2007).
5. Dunn, S., Rush, L., Lu, J-Y., & Xu, T. Mutations in the *Drosophila* tricellular junction protein M6 synergize with RasV12 to induce apical cell delamination and invasion. *Proc Natl Acad Sci U S A*., **115**, 8358–8363 (2018).
6. Maloy, K. J. & Powrie, F. Intestinal homeostasis and its breakdown in inflammatory bowel disease. *Nature*, **474**, 298–306 (2011).
7. Powell, D. W. Barrier function of epithelia, *Am. J. Physiol,* **241**, G275-G288 (1981).
8. King, R. C. & Koch, E. A. Studies on the ovarian follicle cells of *Drosophila, Q. J. Microsc. Sci.*, **104,** 297 320 (1963).
9. Dobens, L. L. & Raftery, L. A. Integration of epithelial patterning and morphogenesis in *Drosophila* ovarian follicle cells, *Dev Dyn*, **218**, 80-93 (2000).
10. DiMario, P. J. & Mahowald, A. E. Female sterile (1) yolkless: A recessive female sterile mutation in *Drosophila melanogaster* with depressed numbers of coated pits and coated vesicles within the developing oocytes. *J. Cell Biol*, **105**, 199-206 (1987).

270 11. Bownes, M., Ronaldson, E., Mauchline, D., & Martinez, A. Regulation of vitellogenesis
271 in *Drosophila*, *International Journal of Insect Morphology and Embryology,* **22**, 349-367
272 (1993).
273 12. Richard, D. S., *et al.* Yolk protein endocytosis by oocytes in *Drosophila melanogaster*:
274 immunofluorescent localization of clathrin, adaptin and the yolk protein receptor, *J.*
275 *Insect Physiol*, **47**, 715–723 (2001).
276 13. Weiner, A. J, Goralsky, T. J., & Mahowald, A. P. The follicle cells are a major site of
277 vitellogenin synthesis in *Drosophila*. *Dev Biol.*, **89**, 225-236 (1982).
278 14. Isaac, P. G. & Bownes, M. Ovarian and Fat-Body Vitellogenin Synthesis in *Drosophila*
279 *melanogaster Eur. J. Biochem*, **123**. 527-534 (1982).
280 15. Tufail, M. & Takeda, M. Insect vitellogenin/lipophorin receptors: Molecular structures,
281 role in oogenesis, and regulatory mechanisms, *J. Insect Physiol.* **55**, 88-104 (2009).
282 16. Herren, J. K., Paredes, J. C., Schüpfer, F., & Lemaitre, B. Vertical transmission of a
283 *Drosophila* endosymbiont via cooption of the yolk transport and internalization
284 machinery. *mBio*. **4(2),** e00532-12 (2013).
285 17. Pratt, G. E. & Davey, K. G. The corpus allatum and oogenesis in *Rhodnius prolixus*
286 (Stål.) 1. Effects of Allatectomy. *J. Exp. Biol.*, **56**, 201-214 (1972).
287 18. Huebner, E. & Injeyan, H. S. Patency of the follicular epithelium in *Rhodnius prolixus*: a
288 re-examination of the hormone response and technique refinement. *Canadian Journal of*
289 *Zoology*, **58**, 1617-1625 (1980).
290 19. Genova, J. L. & Fehon, R. G. Neuroglian, Gliotactin, and the Na+/K+ ATPase are
291 essential for septate junction function in *Drosophila*. *J Cell Biol.*, **161**, 979–989 (2003).

292 20. Jia, D., Xu, Q., Xie, Q., Mio, W., & Deng, W.M. Automatic stage identification of
293 *Drosophila* egg chamber based on DAPI images. *Sci Rep*. **5**, p.12328 (2015).
294 21. French, R. L., Cosand, K. A., & Berg, C. A. The *Drosophila* female sterile mutation twin
295 peaks is a novel allele of tramtrack and reveals a requirement for Ttk69 in epithelial
296 morphogenesis. *Dev. Biol*., **253**, 18-35 (2003).
297 22. Boyle, M. J. & Berg, C. A. Control in time and space: Tramtrack69 cooperates with
298 Notch and Ecdysone to repress ectopic fate and shape changes during *Drosophila* egg
299 chamber maturation. *Development*. **136**, 4187-4197 (2009).
300 23. Neuman-Silberberg, F.S., & Schupbach, T. The *Drosophila* dorsoventral patterning gene
301 Gurken produces a dorsally localized RNA and encodes a TGF alpha-like protein. *Cell,*
302 **75**, 165–174 (1993).
303 24. Twombly, V., *et al.* W.M. The TGF-beta signaling pathway is essential for *Drosophila*
304 oogenesis. *Development,* **122**, 1555–1565 (1996).
305 25. Berg, C.A. The *Drosophila* shell game: patterning genes and morphological change.
306 *Trends Genet*., **21**, 346–355 (2005).
307 26. Sieber, M. H. & Spradling, A. C. Steroid Signaling Establishes a Female Metabolic State
308 and Regulates SREBP to Control Oocyte Lipid Accumulation. *Curr Biol*. **25**, 993–1004
309 (2015).
310 27. Abu-Hakima, R. & Davey, K. G. The action of juvenile hormone on the follicle cells of
311 Rhodnius Prolixus: the importance of volume changes. *J. exp. Biol.*, **69**, 33-44 (1977).
312 28. Davey, K. G., Sevala, V. L., & Gordon, R. B. The action of juvenile hormone and
313 antigonadotropin on the follicle cells of *Locusta migratoria*. *Invest. Reprod. Dev*., **24**, 39-
314 45 (1993).

315 29. Bai, H. & Palli, S. B. Identification of G protein-coupled receptors required for
316 vitellogenin uptake into the oocytes of the red flour beetle, *Tribolium castaneum*. *Sci*
317 *Reports*, **6**, p27648 (2016).
318 30. Postlethwait, J. H. & Handler, A. M. The roles of juvenile hormone and 20-hydroxy-
319 ecdysone during vitellogenesis in isolated abdomens of *Drosophila melanogaster*. *J.*
320 *Insect Physiol*. **25**, 455–460 (1979).
321 31. M. Bownes, The roles of juvenile hormone, ecdysone and the ovary in the control of
322 *Drosophila* vitellogenesis. *J. Insect Physiol.* **35,** 409–413 (1989).
323 32. Byri, S. et al. The Triple-Repeat protein Anakonda controls epithelial tricellular junction
324 formation in *Drosophila*. *Dev Cell*, **33**, 535 – 548 (2015).
325 33. Letizia, A. et al. Sidekick is a key component of tricellular adherens junctions that acts to
326 resolve cell rearrangements. *Dev Cell*, **50**, 313 – 326 (2019).
327 34. Finegan, T. M. et al. The tricellular vertex-specific adhesion molecule Sidekick facilitates
328 polarised cell intercalation during *Drosophila* axis extension. *PloS Biol.*,
329 **17(12)**:e3000522 (2019).
330 35. Uechi, H. & Kuranaga, E. Inhibition of a negative feedback for persistent epithelial cell–
331 cell junction contraction by p21-activated kinase 3. Preprint at doi:
332 https://doi.org/10.1101/743237 (2020)
333 36. Zappia, M. P., Brocco, M. A., Billi, S. C., Frasch, A. C., & Ceriani, M. F. M6 membrane
334 protein plays an essential role in *Drosophila* oogenesis. *PLoS One,* **6(5)**:e19715 (2011).
335 37. Schotman, H., Karhinen, L., & Rabouille, C. dGRASP-mediated noncanonical integrin
336 secretion is required for *Drosophila* epithelial remodeling. *Dev Cell.* **14**, 171-182 (2008).

337 38. Deng, W.M., Althauser, C., & Ruohola-Baker. H. Notch-Delta signaling induces a
338 transition from mitotic cell cycle to endocycle in *Drosophila* follicle cells. *Development*,
339 **128**, 4737-4746 (2001).

340 39. Sun, J.J. & Deng, W.M. Notch-dependent downregulation of the homeodomain gene cut
341 is required for the mitotic cycle/endocycle switch and cell differentiation in *Drosophila*
342 follicle cells. *Development*, **132**, 4299-4308 (2005).

343 40. Tamori, Y., Suzuki, E., & Deng, W.M. Epithelial tumors originate in tumor hotspots, a
344 tissue-intrinsic microenvironment. *PLoS Biol*, **14**: e1002537 (2016).

345 41. Matsumoto, E., Hirosawa, K., Takagawa, K., & Hotta, Y. Structure of retinular cells in a
346 *Drosophila melanogaster* visual mutant, rdgA, at eary stages of degeneration. *Cell Tissue*
347 *Res.,* **300**, 252-293 (1988).

348 42. Wang, C., Guo, X., Dou, K., Chen, H., & Xi, R. Ttk69 acts as a master repressor of
349 enteroendocrine cell specification in *Drosophila* intestinal stem cell lineages.
350 *Development*, **142**, 3321-3331 (2015).

351 43. Carney, G. E. & Bender, M. The *Drosophila* ecdysone receptor (EcR) gene is required
352 maternally for normal oogenesis. *Genetics*, **154**, 1203-1211 (2000).

353

354 **Acknowledgements and funding**

355 We thank Drs. V. Auld, C. Berg, D. Houle, B. Lemaitre, R. Xi, Developmental Studies
356 Hybridoma Bank (DSHB, USA), and Bloomington Drosophila Stock Center (BDSC, USA) for
357 antibodies and fly stocks. We acknowledge the assistance of the UT Southwestern Electron
358 Microscopy Core Facility for acquiring TEM images. We thank members of the Deng laboratory

for valuable discussions and support, and P. Michael Albert II for assistance with editing the manuscript. W.-M. D. is supported by NIH R01 GM072562, R01 CA224381, R01 CA227789 and NSF IOS-1552333.

Author contributions

Conceptualization, methodology, validation, investigation, visualization, project administration: S.R., W.-M.D.; Writing - original draft: S.R.; Writing - review & editing: S.R., W.-M.D.; Supervision, funding acquisition: W.-M.D.

Competing interests

The authors declare no competing interests.

Materials and Correspondence

All data is available in the manuscript or the supplementary materials. Correspondence and material requests should be addressed to Wu-Min Deng at wdeng7@tulane.edu.

Supplementary Information

Figures S1-S5

Figures

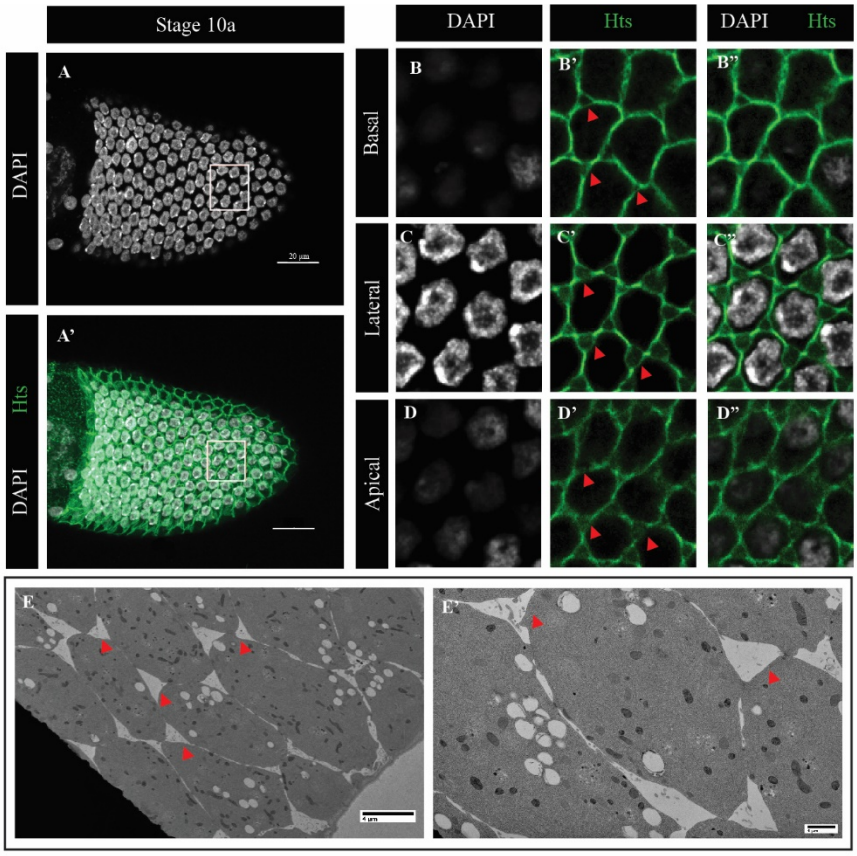

Fig. 1. Patency in *Drosophila melanogaster*. (A-A') Stage 10a oocyte-associated FE. White box is expanded in (B-D"). (B-B", C-C", D-D") Basal, lateral, and apical view, respectively, of the TC gaps in oocyte associated FE at St 10a. Hts (Hu li tai shao, adducin) marks the membrane, DAPI marks the nuclei. (E-E') TEM images of the surface of a St10a FE. TC gaps indicated by red arrowheads.

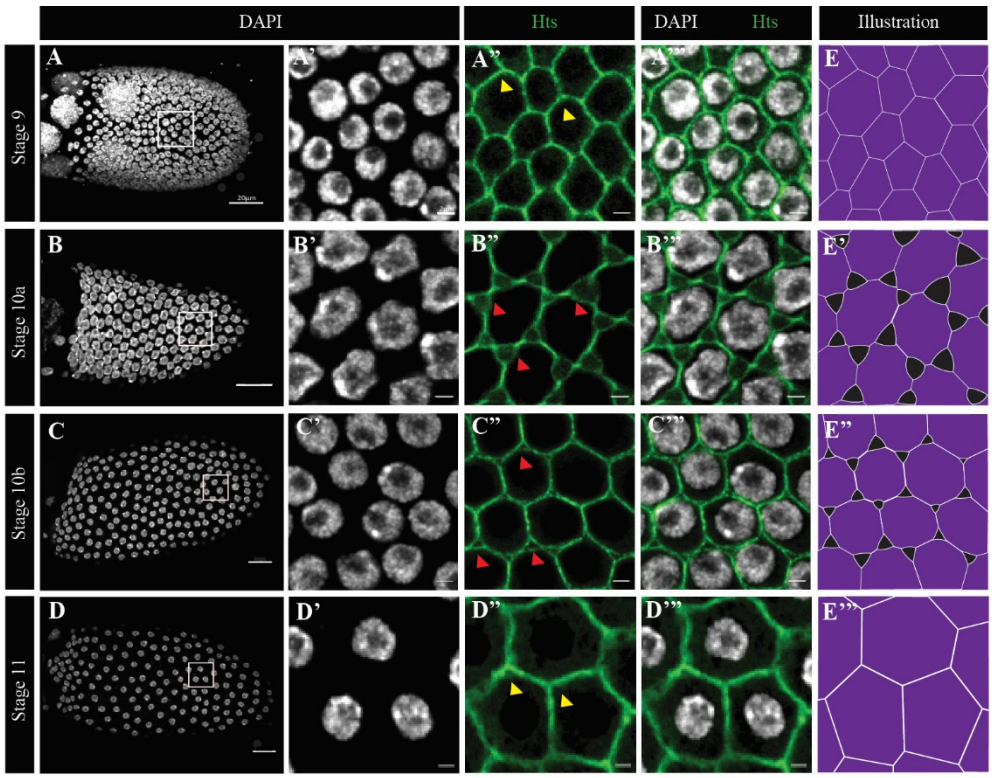

Fig. 2. Temporal range of patency. (A-D) Projections of St9-St11 egg chambers. Regions in the white box are expanded in (A'-A''' to D'-D'''). Intact TCs at stages 9 and 11 (yellow arrowheads in A" and D" respectively), and patent TCs at stages 10a and 10b (red arrowheads in B" and C" respectively). (E-E''') Illustrations of FE at stages 9 through 11 depicting intact and patent TCs. Hts marks the membrane (green) and DAPI marks nuclei.

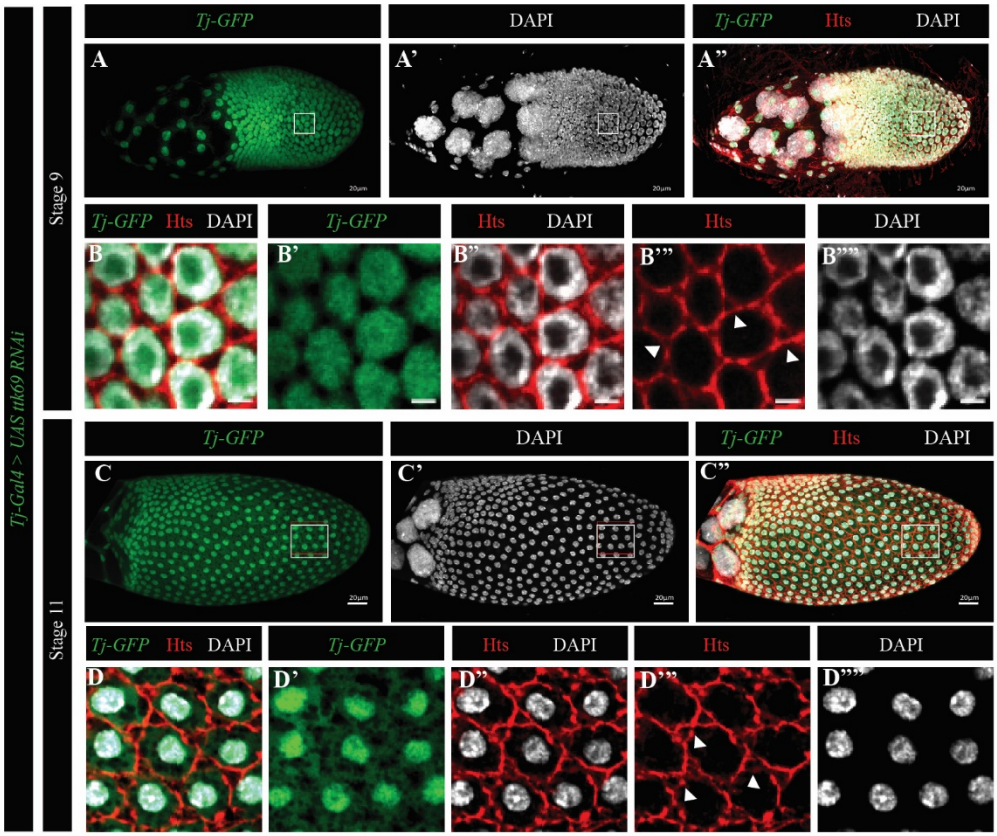

Fig. 3. Ttk69 regulates the temporal range of patency. (A-D'''') *UAS-ttk69-RNAi* expressing FE under *Tj>Gal4*, marked by *UAS-GFP*. ttk69 KD St 9 (A-A") and St 11 (C-C") egg chambers; white boxes are enlarged in (B-B'''') and (D-D'''') respectively, both showing ectopic gaps (white arrowheads). Hts marks the membrane (red), and DAPI marks nuclei.

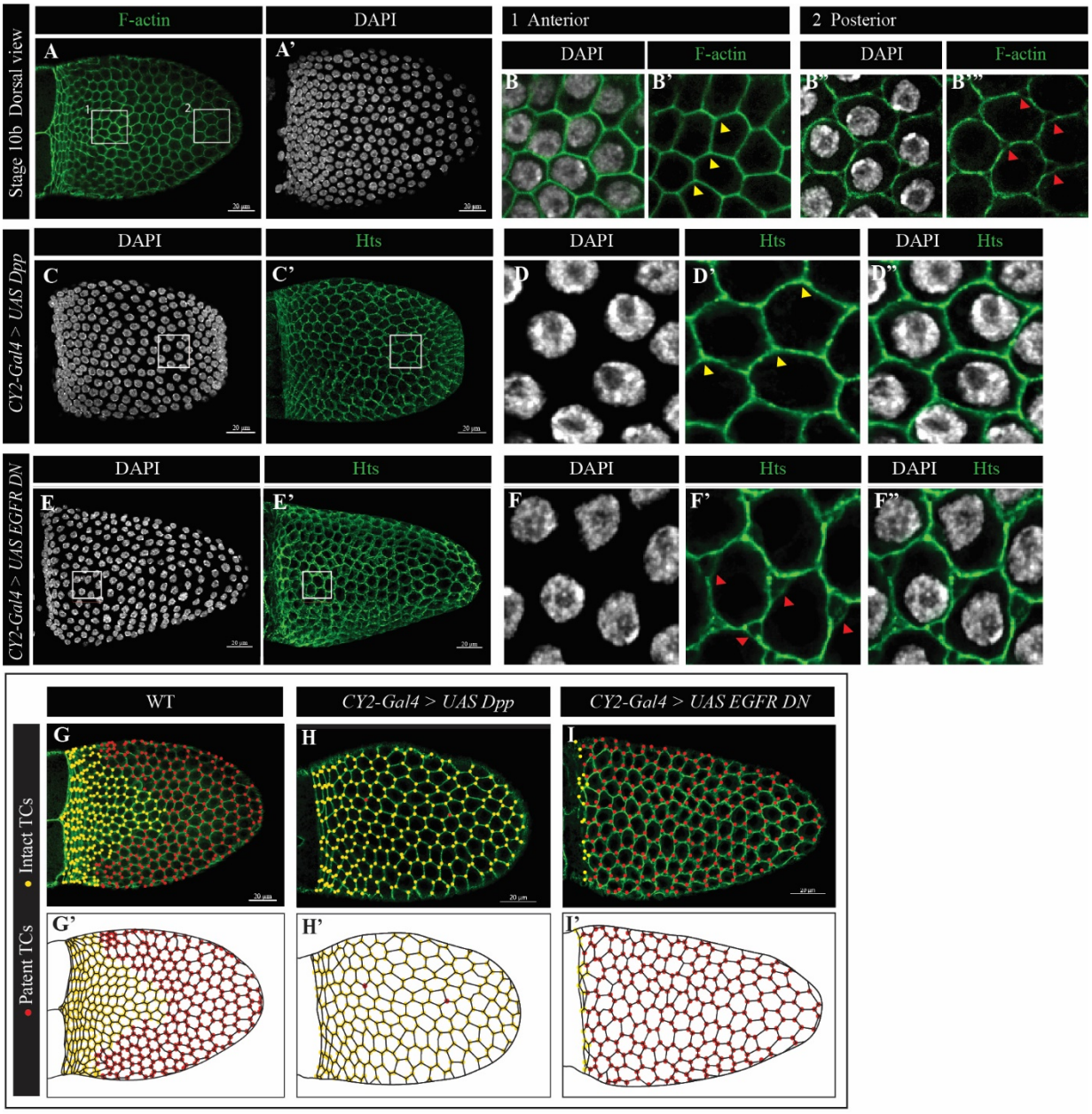

Fig. 4. Spatial pattern of follicular patency and regulation. (A-A") Dorsal view of a St 10b egg chamber. Box#1 in the dorsal-anterior is enlarged in (B-B') showing intact TCs (yellow arrowheads); box#2 in the dorsal posterior is enlarged in (B"-B"') showing patent TCs (red arrowheads). (C-C') Dorsal view of a *UAS-Dpp* expressing FE. White box is enlarged in (D-D") showing absence of patency (yellow arrowheads) (E-E') Dorsal view of *UAS-EGFR-DN* expressing FE. White box is enlarged in (F-F") showing ectopic patency in the dorsal anterior (directly above the oocyte nucleus) (red arrowheads). (G-I') Illustration of the spatial pattern of patency, with yellow dots marking intact TCs , and red dots marking patent TCs in WT (G-G'), *UAS-Dpp* (H-H'), and *UAS-EGFR-DN* (I-I') expressing FE.

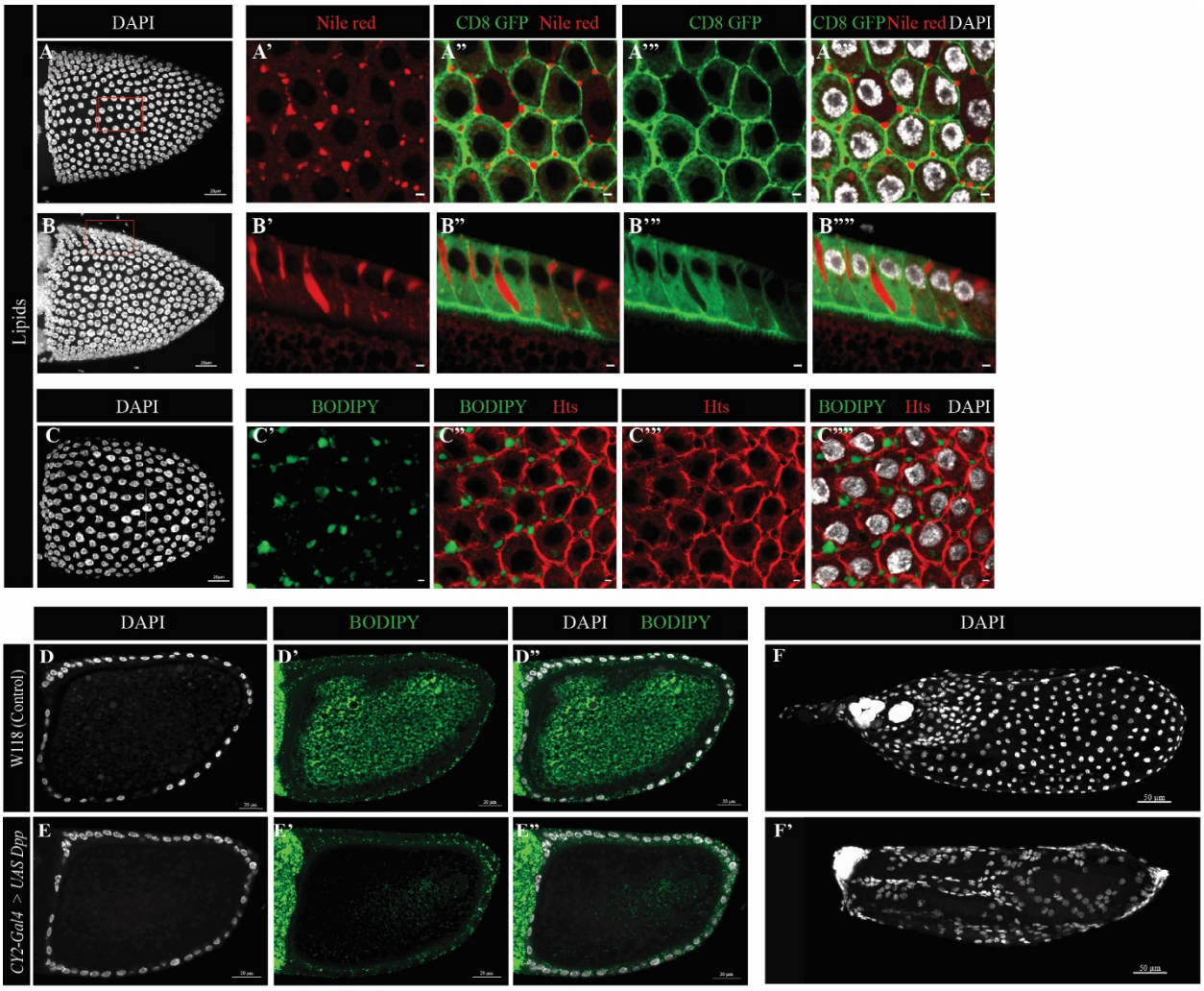

Fig. 5. Patency for lipid uptake by the oocyte at St 10a. (A-C'''') Lipids are present in the gaps in patent FE. (A-B'''') Nile red staining shows lipids in the TC gaps, and spanning the FE. Basal and cross section views (A'-A''''', B'-B''''' respectively). CD8-GFP marks the membrane. (C-C'''') BODIPY493/503 (green) confirms presence of lipids in the gaps. Membrane is marked by Hts (red). BODIPY staining of control WT St 10a egg chamber (D-D'') and *UAS-Dpp* expressing FE lacking patency showing reduced levels of oocyte lipids at St 10a (E-E''). Note FE lipid globules are present in both. (F-F') Later stage egg chambers with (F) WT FE and (F') *UAS-Dpp* expressing FE, resulting in abnormal egg chambers. DAPI marks the nuclei.

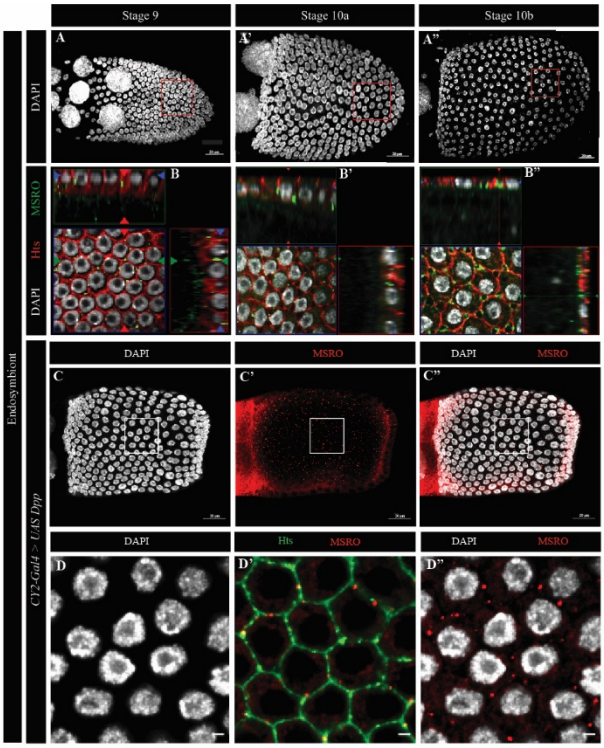

Fig. 6. Vertical transfer of the endosymbiont *Spiroplasma pulsonii* across the FE between stages 9 and 11. (A-A") Projections of DAPI stained Stage 9 – 11 egg chambers. Red boxed are enlarged in (B-B"), and ortho views are provided for top and cross-sectional views. MSRO marks the bacteria, Hts marks the membrane, and DAPI stains the nuclei. (B) The bacteria are seen in the TCs of the FE at St 9 when they are still intact, as well as within the cells. (B'-B") Bacteria are still present within the FE, and now occupy patent TCs at St 10a and 10b. (C-D") MSRO staining in *UAS-Dpp* expressing FE shows the endosymbiont between the cells when the TCs remain intact, similar to WT St 9 with intact TCs.

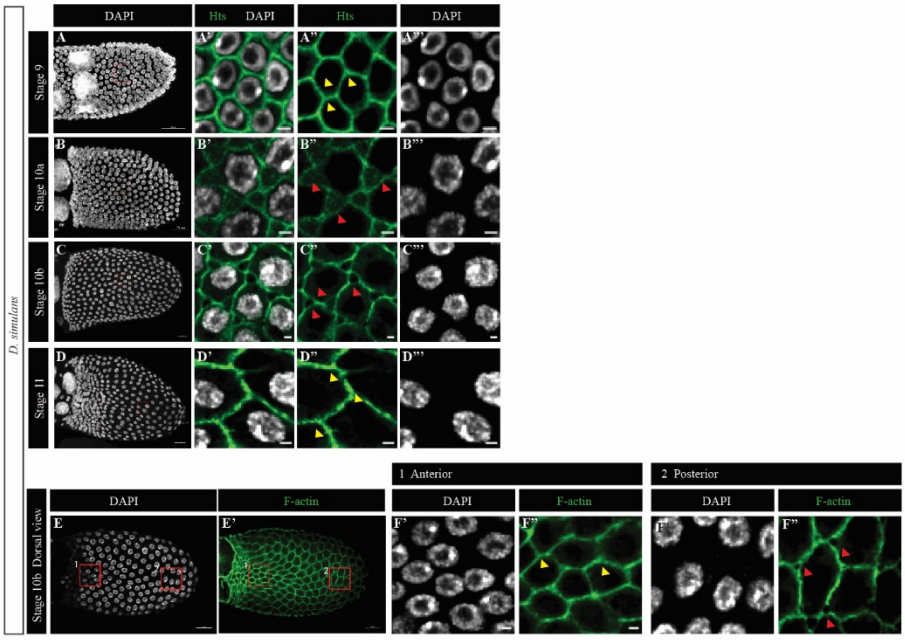

Fig. 7. Temporal range and spatial pattern are conserved in *Drosophila simulans*. (A-D’’’) Temporal range of patency in *D. simulans*. St 10a (B-B’’’) and St 10b (C-C’’’) show TC gaps characteristic of patency, while St 9 (A-A’’’) and St 11(D-D’’’) have intact TCs. (E-F’’) Spatial pattern of patency in *D. simulans* is similar to that in *D. melanogaster*. (E-E’’) Dorsal view of a Stage 10b egg chamber in *D. simulans*. Box 1 in the dorsal anterior is expanded in (F-F’) showing intact TCs (yellow arrowheads). Box 2 in the dorsal posterior is expanded in (F’’-F’’’) showing TC gaps (red arrowheads).

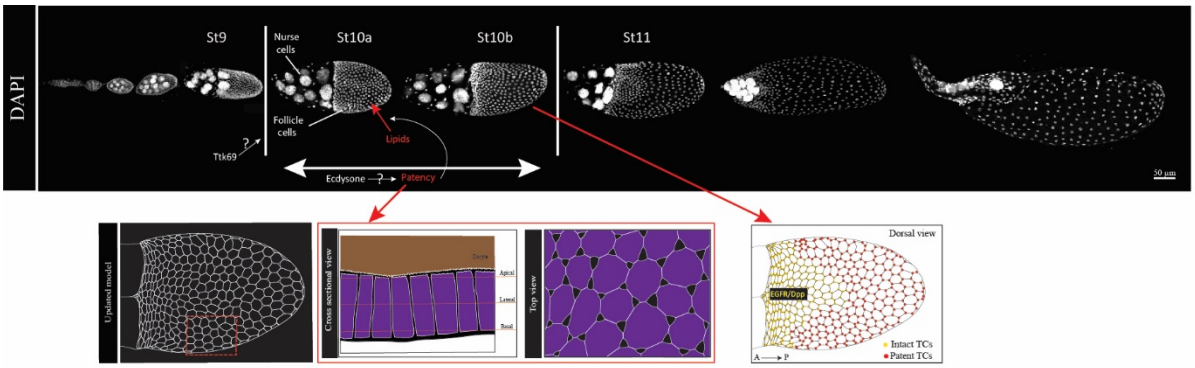

Fig. 8. Model of follicular patency regulation in *Drosophila melanogaster*. DAPI stained egg chambers as arranged in an ovariole, depicting germarium to St 13. Patency is observed in the Oocyte-associated follicular epithelium as gaps between the cells from the basal to the apical domain, illustrated in the cross-sectional and top-down views. The strict temporal range of patency (St10a - 10b) is regulated by Ttk69, and the mechanistic details are yet to be discovered. We also found that Ecdysone signaling - which incidentally becomes activated in the FE at St 10a (*43*) - generates patency, and patency in turn is required for lipid uptake by the oocyte at St 10a. At stage 10b, the dorsalizing signals EGFR and Dpp create a spatial pattern of patency, illustrated as 'intact TCs' at the dorsal anterior, and 'patent TCs' in the rest of the FE.